

## $\delta$ electrons and continuous x rays in heavy-ion—atom collisions

F. Bell, G. Trollmann, H.-D. Betz, and E. Spindler

*Sektion Physik, Universität München, D-8046 Garching, Am Coulombwall 1, West Germany*

(Received 16 October 1981)

Doubly differential cross sections have been measured for the production of 10–70-keV  $\delta$  electrons and  $\sim 10$ –50-keV continuum x rays generated in collisions between 65-MeV nickel ions and nickel foil targets. The data on  $\delta$  electrons have been used to calculate corresponding yields of secondary-electron bremsstrahlung (SEB) including retardation effects. Magnitude, energy, and angular dependence of resulting SEB yields are discussed in detail. It is concluded that SEB contributions do not dominate experimental continuous x-ray spectra.

### INTRODUCTION

Emission of continuous x rays and  $\delta$  electrons in near-adiabatic collisions between heavy ions and target atoms has received much attention particularly in connection with studies of transiently formed superheavy quasiatoms. There has been some hope that x rays which are emitted during ion-atom collisions can be utilized to infer characteristics of combined atoms. For this reason, numerous investigations have been reported of moderately heavy collision systems<sup>1</sup>; for example, in Ni→Ni encounters where  $Z_1=Z_2=28$  one tries to find features in the emission spectra which reflect properties of the combined system with  $Z=56$ .<sup>2</sup>

Unique identification of united-atom effects is not easily achieved. A first important step is to demonstrate that the observed continuous radiation which is not characteristic for projectile or target atoms is indeed emitted from the quasiatom. Since there is no simple distinct feature in the energy spectrum of the continuous radiation, it is difficult to discriminate against various background effects such as secondary-electron bremsstrahlung<sup>3</sup> (SEB), tails from radiative electron capture,<sup>4</sup> nucleus-nucleus bremsstrahlung,<sup>5</sup> and other higher-order effects. An interesting technique consists in a Doppler-shift analysis of the continuous radiation<sup>2,6–9</sup> in order to determine the effective velocity of the emitting system. In many cases, this velocity was found to be close to the center-of-mass velocity of the colliding system, giving strong evidence for a combined-atom origin of the radiation. The difficulty with this technique, though, is that it relies on measured forward-backward asymmetry of emitted continuous radiation which does not represent a unique signature for united-atom effects, because it can also be caused by SEB provided that retardation

effects are taken into account.

The main purpose of this paper is to demonstrate to what extent SEB contributes to continuous spectra and what kind of angular distribution arises from SEB. These results are essential for a full validation of the Doppler-shift analysis of continuous radiation. Our technique is to measure doubly differential cross sections for  $\delta$  electrons, which are difficult to calculate for heavy homonuclear systems, and to compute the corresponding SEB yields on the basis of well-developed procedures, including retardation effects. A point of major concern is the forward-backward asymmetry of SEB which is shown to be indeed pronounced in the system studied here. We find, however, that the magnitude of SEB is not sufficient to explain the observed continuous radiation and that the angular distribution of SEB is not symmetrical with respect to forward-backward angles in the center-of-mass system, contrary to what one expects for radiation from transiently combined atomic systems.

### EXPERIMENTAL PROCEDURE

The Munich tandem Van de Graaff accelerator was used to study production of  $\delta$  electrons and x rays in collisions between 65-MeV nickel ions and nickel targets. Doubly differential cross sections for  $\delta$ -electron production were measured for electron energies between 10 and 70 keV and ejection angles from  $5^\circ$  to  $180^\circ$ . Targets were oriented perpendicular to the beam direction; target thickness was typically  $130 \mu\text{g}/\text{cm}^2$ . Electron deflection was achieved by a liquid-nitrogen-cooled iron-free solenoid with magnetic fields up to 50 mT, momentum resolution of 4%, and angular acceptance of  $\sim 3$  msr. Electrons were detected with a cooled sur-

face barrier detector. The total detection efficiency of the solenoid was calibrated by means of conversion electron sources of known activity. A more detailed description of the electron detection can be obtained elsewhere.<sup>10</sup> At the same beam energy, but using a 200- $\mu\text{g}/\text{cm}^2$  nickel target oriented at 45° with respect to beam direction, we recorded x-ray spectra at 90° with a Si (Li) detector in the range  $\leq 50$  keV. Solid angle and efficiency were carefully determined. Beam normalization was achieved by means of a Faraday cup and known average charge state of the ions behind the target foil. Resulting absolute electron and x-ray cross sections have an estimated uncertainty of  $\sim 30\%$ . Our x-ray cross sections agree with the ones from Ref. 11 within  $\sim 30\%$ .

### δ-ELECTRON SPECTRA

At all  $\delta$ -electron energies  $E_e$  the measured angular distributions show strong forward peaking in the laboratory system. Transformation to the center-of-mass (c.m.) system is achieved by means of

$$\frac{d^2\sigma}{dE'_e d\Omega'_e} = \frac{p'}{p} \frac{d^2\sigma}{dE_e d\Omega_e} \quad (1)$$

and the relativistic velocity addition theorem. In Eq. (1) unprimed and primed variables refer to laboratory and c.m. systems, respectively, and  $p$  denotes the momentum of the electron. Application to our data yields c.m. contributions which exhibit forward-backward symmetry as is expected for a symmetric collisions system (see the solid line in Fig. 1). Although the c.m. velocity is roughly an order of magnitude smaller than the electron velocity (a factor of  $\sim 13$  for 25-keV electrons), the transformation effect is remarkable. This can be understood in view of the strong  $E_e$  dependence of the cross section; between 15 and 40 keV, the  $\delta$ -electron cross section is found to be proportional to  $E_e^{-8.7}$ . Therefore, small changes in  $E_e$  which arise from the transformation can lead to significant changes of the cross section. Detailed results on doubly differential cross sections for production of  $\delta$  electrons in heavy collision systems will be published separately.<sup>10,12</sup>

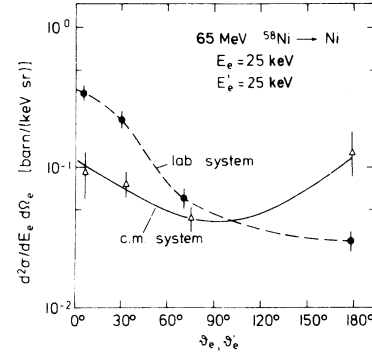


FIG. 1. Angular distribution of 25-keV  $\delta$  electrons emitted in 65-MeV  $^{58}\text{Ni}$ -Ni collisions in the laboratory (dashed line) and c.m. systems (solid line). Note that the c.m. distribution exhibits forward-backward symmetry.

### COMPUTATION OF SEB SPECTRA

For a given  $\delta$ -electron distribution  $d^2\sigma/dE_e d\Omega_e$ , a quite rigorous calculation of the corresponding SEB spectrum would be feasible if one need not to worry about energy loss and scattering of the electrons in the target foil. In order to keep computational efforts small, we considered the following two extreme simplifications:

- (i) neglecting the energy loss of  $\delta$  electrons in the target;
- (ii) stopping  $\delta$  electrons within the target.

Assumption (i) seems justified for these electrons which move perpendicular to the foil surface when one takes into account that the foil thicknesses used are thin compared to the range of  $\delta$  electrons considered here. We expect that correct SEB yields lie somewhere between results from (i) and (ii), obtained from

$$\frac{d^2\sigma^{\text{SEB}}}{dE_x d\Omega_x} = N \frac{x_0}{2} \int d\Omega_e \int_{E_x}^{\infty} dE_e \frac{d^2\sigma}{dE_e d\Omega_e} \times \frac{d^2\sigma^{\text{B}}(E_e, E_x)}{dE_x d\Omega_x} \quad (2)$$

for case (i) and, for case (ii),

$$\frac{d^2\sigma^{\text{SEB}}}{dE_x d\Omega_x} = \int d\Omega_e \int_{E_x}^{\infty} dE_e \frac{d^2\sigma}{dE_e d\Omega_e} \int_{E_x}^{E_e} \frac{dE'_e}{S(E'_e)} \frac{d^2\sigma^{\text{B}}(E'_e, E_x)}{dE_x d\Omega_x}, \quad (3)$$

where  $x_0$ ,  $E_e$ , and  $E_x$  denote target thickness, electron, and x-ray energy, respectively,  $S(E_e)$  stands for elec-

tron stopping power, and  $d^2\sigma^B$  signifies the doubly differential cross section for bremsstrahlung. For the latter, we use<sup>13</sup>

$$\frac{d^2\sigma^B(E_x, E_e)}{dE_x d\Omega_x} = \frac{3}{8\pi} C_1 \frac{Z_t^2}{E_e E_x} \left[ \frac{2P}{3-P} \lambda^4 \sin^2\varphi + \lambda^2 \frac{2(1-P)}{3-P} \right], \quad (4)$$

where  $C_1 = 1.44$  keV b,  $Z_t$  is the nuclear charge of target,  $P$  the polarization of the bremsstrahlung,  $\varphi$  the angle between directions of electron momentum and x-ray emission, and  $\lambda = (1 - \beta \cos\varphi)^{-1}$  (with  $\beta = v_e/c$ ) a retardation factor.<sup>14</sup> Polarization is given by<sup>13</sup>

$$P = \frac{6K + (1 - 3K^2) \ln \left[ \frac{1+K}{1-K} \right]}{2K + (3 - K^2) \ln \left[ \frac{1+K}{1-K} \right]}, \quad (5)$$

where  $K^2 = 1 - E_x/E_e$ . When we evaluate the single differential bremsstrahlung cross section  $d\sigma^B/dE_x$  we find agreement within  $\sim 15\%$  with the most refined nonrelativistic quantum-mechanical calculations available.<sup>15</sup>

Electronic stopping is conveniently represented by<sup>16</sup>

$$S(E_e) = \frac{1}{N} C_2 \frac{Z_t}{E_e}, \quad C_2 = 6 \times 10^5 \quad (6)$$

in units of keV<sup>2</sup> b/atom.

Utilizing our doubly differential cross sections for  $\delta$ -electron production we have evaluated Eqs. (2) and (3). In the range of present interest,  $15 \text{ keV} \lesssim E_x \lesssim 40 \text{ keV}$ , we find that SEB yields based on case (i) are 3–4 times larger than those based on case (ii), independent of the x-ray detection angle. Our results from case (ii) are illustrated in Fig. 2 and represent an upper limit for the SEB magnitude.

It is worthwhile to explain why the SEB yield from (ii) is smaller than the one which results from approximation (i) even though relatively thin foils are used; for 25-keV electrons, for example, Eq. (6) gives a range in nickel of  $\sim 1.8 \text{ mg/cm}^2$  which must be compared with a foil thickness  $0.2 \text{ mg/cm}^2$ . This behavior originates in the steepness of cross sections  $d\sigma(E_e)/dE_e$ : even small energy loss of a  $\delta$  electron with initial energy  $E_e$  renders this electron ineffective for further production of bremsstrahlung, since many more electrons are available with initial energies below  $E_e$ . Obviously, consideration of electron ranges can be misleading. In this connection, it becomes clear that SEB is not easily discriminated against other radiation sources by

means of target thickness variation: Since SEB is produced by a two-step process it is often assumed that SEB yields are proportional to the square of target thickness,  $x_0^2$ . The necessary condition for such a behavior is *not*  $x_0 \ll E_x/(dE_e/dx)$ , but  $x_0 \ll E_x/n(dE_e/dx)$ , where  $n$  is the usually large exponent in the energy dependence of the  $\delta$ -electron cross section.

Two further approximations must be discussed which are involved in Eqs. (2) and (3). First, angular scattering of  $\delta$  electrons has been neglected. Such an effect would tend to smear out the directional anisotropy of SEB. We checked this experimentally and measured the  $\delta$ -electron yield as a function of target thickness. For foil thicknesses of present interest a linear dependence was found which reveals that scattering effects are not influential. Second, we assumed an average bremsstrahlung production length  $x_0/2$  in Eq. (2), and neglect-

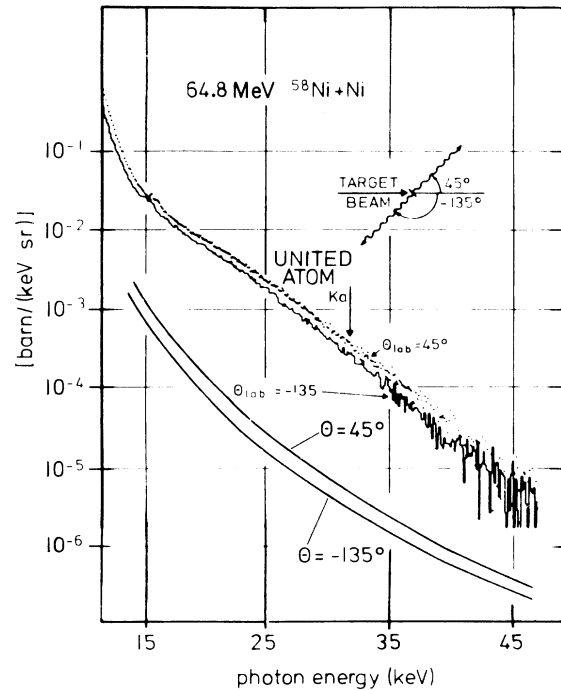


FIG. 2. Comparison between experimental continuum x rays from Ref. 2 (upper curves) and our SEB spectrum (lower solid lines). Both cases exhibit forward-backward asymmetry.

ed path length changes for electrons moving at large angles with respect to the beam direction. We argue that this is justified due to the strong forward peaking of the electrons in the laboratory system (Fig. 1).

### DISCUSSION OF RESULTS

Figure 2 shows the comparison between absolute SEB production and experimental x-ray spectra for observation angles  $45^\circ$  and  $135^\circ$  between directions of x-ray observation and beam propagation. The absolute x-ray data originates from Refs. 2 and 11 whereby we took into account the anisotropy of the continuous radiation. In addition, the absolute yield was confirmed by our x-ray data which agreed with the yield from Ref. 11 within  $\sim 30\%$ . It becomes obvious that especially the magnitude of SEB contributions does not explain the experimental x-ray data. SEB is more than 1 order of magnitude less intense, though spectral shape and forward-backward asymmetry at  $45^\circ$  and  $135^\circ$  exhibit surprisingly similar behavior.

Full angular distributions for SEB and experimental continuous radiation are displayed in Fig. 3. Some of the distributions are displayed in the c.m. system where forward-backward symmetry for  $\delta$  electrons and molecular-orbital (MO) radiation is expected on the basis of symmetry arguments. The effect of transformation from laboratory (curve a) to c.m. system (curve b) is shown for SEB when retardation is neglected. A small directional anisotropy is obtained,  $I(90^\circ)/I(0^\circ) \cong 1.15$ , because the  $\delta$ -

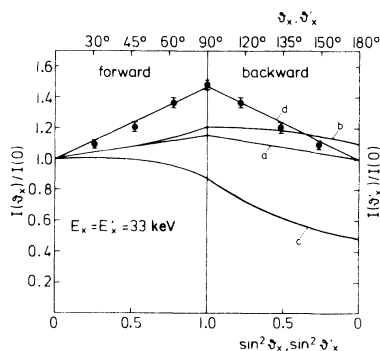


FIG. 3. Angular distribution of continuum x rays for 33-keV photon energy, obtained for 65-MeV  $^{58}\text{Ni}$ -Ni collisions. Curve a: Theoretical SEB spectrum in the laboratory frame, retardation neglected; curve b: the same as "a", but transformed to the c.m. frame; curve c: SEB angular distribution in the c.m. frame with retardation included; curve d: experimental angular x-ray distribution (Ref. 2) in the c.m. frame.

electron distribution is not too different from the form  $1 + b \cos \vartheta_e$  (Fig. 1). For the latter distribution, the formalism in Ref. 17 can be used to show that Eq. (3) gives an isotropic SEB distribution.<sup>18</sup> We note that all SEB calculations shown in Fig. 3 were based on case (ii) from above in order to obtain the largest possible angular anisotropies: when energy loss of  $\delta$  electrons is included, tip bremsstrahlung with maximum polarization is favored somewhat compared with case (i). Nevertheless, the broad angular distribution of electrons does not result in large anisotropies. By contrast, when  $\delta$  electrons in forward direction only were present, a ratio  $I(90^\circ)/I(0^\circ) \cong 15$  would result in the laboratory system. With realistic  $\delta$ -electron distributions, large directional and forward-backward anisotropies of SEB arise only when retardation is included (curve c). Comparison between curve c and the distribution of experimental continuous radiation (curve d) demonstrate again, in line with intensity considerations from above, that SEB cannot account for the observed radiation; the full angular distributions show much better than a single forward-backward intensity ratio that SEB does not yield the symmetric distribution expected for radiation of quasimolecular origin.

### QUASIMOLECULAR AUGER ELECTRONS

Since we have measured both doubly differential cross sections for  $\delta$  electrons and x rays,  $d^2\sigma_e$  and  $d^2\sigma_x$ , respectively, it may be asked whether the results give any indication for a possible molecular origin of  $\delta$  electrons,<sup>19,20</sup> analogous to continuous x rays. In Fig. 4 we plot the branching ratio  $\omega = d^2\sigma_x / (d^2\sigma_x + d^2\sigma_e)$  for c.m. cross sections for  $E'_e = E'_x = 25$  keV as a function of the correspond-

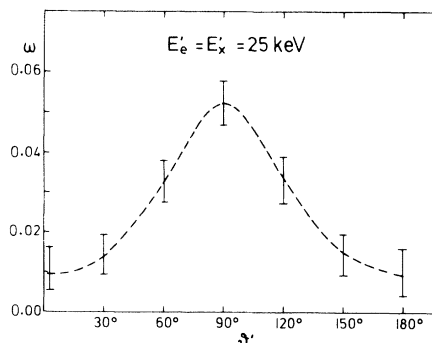


FIG. 4. Absolute values and angular distribution of effective "fluorescent yield"  $\omega$  as defined in text.

ing emission angle in the c.m. system. The maximum value obtained is  $\omega \cong 0.05$ ; in a static system with  $Z \cong 56$  and  $K$ -shell binding near  $\sim 25$  keV one finds  $\omega_K \cong 0.83$ .<sup>21</sup> While some reduction of Auger

rates in a dynamic collision system might be possible, the strong angular dependence of  $\omega$  does not seem to be in accord with the concept of the molecular autoionization states.

- 
- <sup>1</sup>See, for example, the recent review by P. H. Mokler and F. Folkmann, in *Topics in Current Physics*, edited by I. A. Sellin (Springer, Berlin, 1978), p. 201.
- <sup>2</sup>P. Vincent, C. K. Davis, and J. S. Greenberg, *Phys. Rev. A* **18**, 2978 (1978).
- <sup>3</sup>F. Folkmann, C. Gaarde, T. Huss, and K. Kemp, *Nucl. Instrum. Methods* **116**, 487 (1974).
- <sup>4</sup>E. Spindler, H.-D. Betz, and F. Bell, *J. Phys. B* **9**, L1 (1977).
- <sup>5</sup>H. P. Trautvetter, J. S. Greenberg, and P. Vincent, *Phys. Rev. Lett.* **37**, 202 (1976).
- <sup>6</sup>W. E. Meyerhof, T. K. Saylor, and R. Anholt, *Phys. Rev. A* **12**, 2641 (1975).
- <sup>7</sup>W. Frank, K. H. Kaun, P. Manfrass, N. V. Pronin, and Yu. P. Tretyakov, *Z. Phys. A* **279**, 213 (1976).
- <sup>8</sup>F. Folkmann, P. Armbruster, S. Hagmann, G. Kraft, P. H. Mokler, and H. J. Stein, *Z. Phys. A* **276**, 15 (1976).
- <sup>9</sup>Ch. Stoller, E. Morenzoni, W. Wölfli, W. E. Meyerhof, F. Folkmann, P. Vincent, P. H. Mokler, and P. Armbruster, *Z. Phys. A* **297**, 93 (1980).
- <sup>10</sup>F. Bell, G. Trollmann, H. Böckl, and H.-D. Betz, *Nucl. Instrum. Methods* **194**, 423 (1982).
- <sup>11</sup>P. Vincent and J. S. Greenberg, *J. Phys. B* **12**, L641 (1979).
- <sup>12</sup>F. Bell, G. Trollman, and H.-D. Betz, *Phys. Lett.* **88A**, 37 (1982).
- <sup>13</sup>H. A. Bethe and E. E. Salpeter, *Handbuch der Physik*, edited by S. Flügge (Springer, Berlin, 1957), Vol. 35, p. 88.
- <sup>14</sup>M. Scheer and E. Zeitler, *Z. Phys.* **140**, 642 (1955).
- <sup>15</sup>R. H. Pratt, H. K. Tseng, C. M. Lee, L. Kissel, C. McCallum, and M. Riley, *At. Data Nucl. Data Tables* **20**, 175 (1977).
- <sup>16</sup>L. Pages, E. Bertel, H. Joffre, and L. Sklavenitis, *At. Data* **4**, 1 (1972).
- <sup>17</sup>K. Ishii, M. Kamiya, K. Sera, S. Morita, and T. Tawara, *Phys. Rev. A* **15**, 2126 (1977).
- <sup>18</sup>For a  $\delta$ -electron distribution  $1 + b \cos^2 \vartheta_e$ , Vincent *et al.* (Ref. 2) claim erroneously a directional anisotropy for SEB of  $I(90^\circ)/I(0^\circ) - 1 \cong 150\%$ ; isotropy, however, is readily derived from Ref. 17 by means of Eq. (2) and other unnumbered equations on p. 2128, provided one inserts  $\langle \cos^2 \vartheta_e \rangle = \frac{1}{3}$  which holds for the distribution under discussion.
- <sup>19</sup>V. V. Afrosimov, Yu. S. Gordeev, A. N. Sinoviev, A. A. Korotov, and A. P. Shergin, in *Abstracts of the tenth ICPEAC, Paris, 1977*, edited by M. Barat and J. Reinhardt (Commissariat à l'Énergie Atomique, Paris, 1977), p. 924.
- <sup>20</sup>Yu. S. Gordeev, P. H. Woerlee, H. de Waard, and F. W. Saris, *J. Phys. B* **14**, 513 (1981).
- <sup>21</sup>M. O. Krause, *J. Phys. Chem. Ref. Data* **8**, 307 (1979).